https://doi.org/10.5194/bg-2021-324
Preprint. Discussion started: 16 December 2021

Biogeosciences Discussions

Determination of respiration and photosynthesis fractionation coefficients for atmospheric dioxygen inferred from a vegetation-soil-atmosphere analog of the terrestrial biosphere in closed chambers

Clémence Paul[1], Clément Piel[2], Joana Sauze[2], Nicolas Pasquier[1], Frédéric Prié[1], Sébastien Devidal[2], Roxanne Jacob[1], Arnaud Dapoigny[1], Olivier Jossoud[1], Alexandru Milcu[2,3], Amaëlle Landais[1]

[1] Laboratoire des Sciences du Climat et de l'Environnement, LSCE/IPSL, CEA-CNRS-UVSQ, Université Paris-Saclay, 91191 Gif-sur-Yvette, France
[2]Ecotron Européen de Montpellier (UAR 3248), Univ Montpellier, Centre National de la Recherche Scientifique (CNRS), Campus Baillarguet, Montferrier-sur-Lez, France
[3]Centre d'Ecologie Fonctionnelle et Evolutive, Univ Montpellier, CNRS, Univ Paul Valéry, EPHE, IRD, Montpellier, France

Correspondence: Clémence Paul (clemence.paul@lsce.ipsl.fr)

Abstract

The isotopic composition of dioxygen in the atmosphere is a global tracer which depends on the biosphere flux of dioxygen toward and from the atmosphere (photosynthesis and respiration) as well as exchanges with the stratosphere. When measured in fossil air trapped in ice cores, the relative concentration of ^{16}O, ^{17}O and ^{18}O of O_2 can be used for several applications such as ice core dating and past global productivity reconstruction. However, there are still uncertainties about the accuracy of these tracers as they depend on the integrated isotopic fractionation of different biological processes of dioxygen production and uptake, for which we currently have very few independent estimates. Here we determined the respiration and photosynthesis fractionation coefficients for atmospheric dioxygen from experiments carried out in a replicated vegetation-soil-atmosphere analog of the terrestrial biosphere in closed chambers with growing *Festuca arundinacea*. The values for ^{18}O discrimination during soil respiration and dark respiration in leave are equal to -12.3 ± 1.7 ‰ and -19.1 ± 2.4 ‰, respectively. We also found a value for terrestrial photosynthetic fractionation equal to +3.7 ± 1.3 ‰. This last estimate suggests that the contribution of terrestrial productivity in the Dole effect may have been underestimated in previous studies.

https://doi.org/10.5194/bg-2021-324
Preprint. Discussion started: 16 December 2021

1. Introduction

The oxygen cycle represents the most important biogeochemical cycle on Earth: oxygen is the second most important gaseous component in the atmosphere. Oxygen is an essential component for life on Earth as it is consumed by all aerobic organisms through respiration and produced by autotrophic organisms through photosynthesis.

The analysis of the oxygen isotopic composition classically expressed as $\delta^{18}O$ and $\delta^{17}O$ of O_2 in air bubbles trapped in ice cores is currently used to provide information on the variations of low latitude water cycle and the productivity of the biosphere during the Quaternary (Bender et al., 1994; Luz et al., 1999; Malaizé et al., 1999; Severinghaus et al., 2009; Blunier et al., 2002; Landais et al., 2010). $\delta^{18}O$ of O_2 is also a very useful proxy for ice core dating through the resemblance of its variations with the variations of precession or summer insolation in the northern hemisphere (Shackleton, 2000; Dreyfus et al., 2007). These tracers are however complex and their interpretation relies on the precise knowledge of the fractionation factors in the oxygen cycle.

First, the interpretation of variations of $\delta^{18}O$ of O_2 (or $\delta^{18}O_{atm}$) in the old air trapped in ice core in term of low latitude water cycle (e.g. Severinghaus et al., 2009; Landais et al., 2010; Seltzer et al., 2017) is still debated because of the multiplicity of the processes involved. Dole et al. (1954) has shown that the $\delta^{18}O_{atm}$ is enriched compared to the $\delta^{18}O$ of water of the global ocean (taken here as the Vienna Standard Mean Ocean Water, VSMOW) with a value of 23.88 ‰ (Barkan and Luz, 2005). This Dole effect is the result of several fractionations in the biosphere that enrich the $\delta^{18}O_{atm}$ relative to the oceanic one. First measurements have shown that the photosynthesis itself is not associated with a strong fractionation and produces oxygen with an isotopic composition which is close to the isotopic composition of the consumed water (Guy et al., 1993). For the oceanic biosphere, the isotopic composition of O_2 produced by photosynthesis is very close to the isotopic composition of the ocean. However, in terrestrial biosphere the $\delta^{18}O$ of water consumed by photosynthesis (leaf water) is highly variable both spatially and temporally because of the decrease of $\delta^{18}O$ of meteoric water toward higher latitudes and the enrichment in heavy isotopes in leaf water during evaporation. The enrichment of the mean leaf water isotopic composition has been estimated within 4.5 – 6 ‰ with respect to the isotopic composition of the mean global ocean (Bender et al., 1994; Hoffmann et al., 2004). On top of this enrichment, the terrestrial and oceanic Dole effects are mostly explained by the respiratory isotopic discrimination of the order of magnitude of + 18 ‰ (Bender et al., 1994).

Because of the isotopic enrichment in leaf water, the terrestrial Dole effect has been initially estimated to be 5 ‰ higher than the oceanic Dole effect and $\delta^{18}O_{atm}$ used to estimate changes in the balance between land and marine productivity (Wang et al., 2008; Bender et al., 1994; Hoffmann et al., 2004).

https://doi.org/10.5194/bg-2021-324
Preprint. Discussion started: 16 December 2021


Biogeosciences
Discussions
Open Access
EGU

However, the evidence by Eisenstadt et al. (2010) of isotopic discrimination up to + 6‰ for marine phytoplankton photosynthesis rather suggests that the marine and terrestrial Dole effects are of the same order of magnitude. In this case, the past variations of $\delta^{18}O_{atm}$ would be related to low latitude water cycle influencing the leaf water $\delta^{18}O$ consumed by photosynthesis (most important in the low latitude vegetated regions). This is supported by orbital and millennial variations of $\delta^{18}O_{atm}$ in phase with calcite $\delta^{18}O$ in Chinese speleothem, a proxy strongly related to the intensity of hydrological cycle in the South-East Asia (Severinghaus et al., 2009; Landais et al., 2010; Extier et al., 2018). The aforementioned studies show that qualitative and quantitative interpretation of $\delta^{18}O_{atm}$ relies strongly on the estimate of O_2 fractionation factors in the biological cycle but data to constrain the fractionation factors associated with respiration and photosynthesis for the different ecosystems are sparse.

In addition to the use of $\delta^{18}O_{atm}$, the combination of $\delta^{17}O$ and $\delta^{18}O$ of O_2 provides a way to quantify variations in past global productivity (Luz et al., 1999). This method relies on the fact that O_2-fractionating processes in the stratosphere and within the biosphere lead to different relationships between $\delta^{17}O$ and $\delta^{18}O$ of O_2. The biosphere fractionating processes are mass-dependent such that the ^{17}O enrichment is about half the ^{18}O enrichment relative to ^{16}O. On the contrary, oxygen is fractionated in a mass-independent manner in the stratosphere producing approximately equal ^{17}O and ^{18}O enrichments (Luz et al., 1999). We thus define a $\Delta^{17}O$ anomaly as:

$$\Delta^{17}O = \ln(1 + \delta^{17}O) - 0.516 \times \ln(1 + \delta^{18}O) \quad (1)$$

$\Delta^{17}O$ of O_2 is equal to 0 by definition in the present-day troposphere (the standard for isotopic composition of atmospheric oxygen is the present-day atmospheric value). $\Delta^{17}O$ of O_2 is negative in the stratosphere and increase in biosphere productivity leads to an increase of $\Delta^{17}O$ of O_2. As for the interpretation of $\delta^{18}O_{atm}$, the quantitative link between $\Delta^{17}O$ of O_2 and biosphere productivity depends on the exact fractionation factors associated with biosphere processes (Brandon et al., 2020).

Several studies have been conducted to estimate the fractionation factors during biosphere processes of O_2 production and consumption. These fractionation factors are then implemented in global modeling approaches involving the use of models of global vegetation and oceanic biosphere for interpretation of $\Delta^{17}O$ of O_2 and $\delta^{18}O_{atm}$ in term of environmental parameters (Landais et al., 2007; Blunier et al., 2012; Reutenauer et al., 2015; Brandon et al., 2020). Most of the fractionation factors used in these modeling approaches were obtained from studies conducted at the cell level: cyanobacterium (Helman et al., 2005), *E. coli* (Stolper et al., 2018), microalgae (Eisenstadt et al., 2010).

https://doi.org/10.5194/bg-2021-324
Preprint. Discussion started: 16 December 2021

In these studies, the underlying assumption is that the fractionation factor associated with O_2 measured at the cell level can be applied at the ecosystem scale. Yet, results from studies conducted at a larger scale, e.g. at the soil scale by Angert et al. (2001) found a global terrestrial respiratory $^{18}O/^{16}O$ of O_2 discrimination for soil microorganisms varying between - 12 ‰ and - 15 ‰. This is lower than the - 18 ‰ discrimination classically used for respiration, with diffusion in soil playing a role in addition to biological respiration fractionation. Later, Angert et al. (2003) found an even larger spread of O_2 isotopic discrimination in soil and showed that temperate and boreal soils have higher fractionation, respectively - 17.8 ‰ and -22.5 ‰, because they engage the AOX (alternative oxidase) pathway which strongly discriminates ^{18}O, unlike tropical soils (- 10.8 ‰). These contrasting results show the interest of making measurements at a larger scale than at the cell level to correctly interpret global variations of the isotopic composition of oxygen.

In this study we developed a vegetation-soil-atmosphere simplified analog of the terrestrial biosphere in closed chamber of 120 liters with the aim of estimating the fractionation coefficients of atmospheric dioxygen due to soil respiration, plant respiration and photosynthesis. With this setup we carried out several experimental runs with soil only and soil with plants in order to estimate the fractionation of the different compartments and check values obtained at the cell level. The implications for our interpretation of the Dole effect are also discussed.

2.Material and Methods

2.1. Growth chamber and closed system

2.1.1. Plant growth and experimental setup

a)

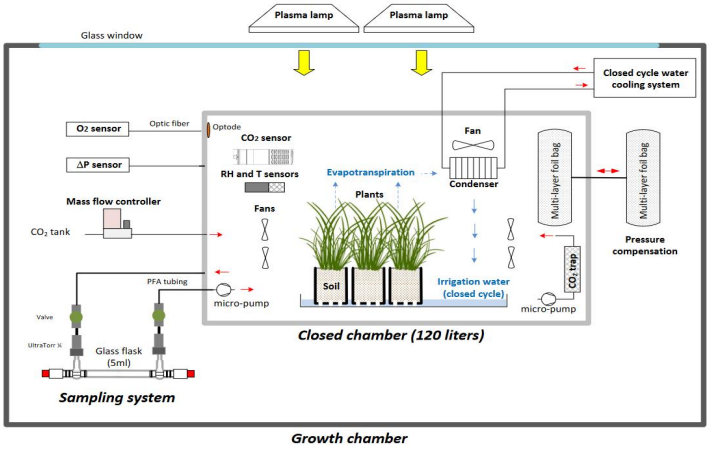

https://doi.org/10.5194/bg-2021-324
Preprint. Discussion started: 16 December 2021

120 **b)**

121

122 **Fig.1. A vegetation-soil-atmosphere analog of the terrestrial biosphere in closed chamber. (a)**
123 **Schematic of the closed chamber setup used for the terrestrial biosphere model.** The 120 liters gas
124 tight closed chamber containing a terrestrial biosphere analogue is enclosed in a larger growth
125 chamber from the Ecotron Microcoms platform. Main environmental parameters inside the closed
126 chamber are actively controlled and monitored: temperature (T), light intensity, CO_2, relative humidity
127 (RH), pressure differential (ΔP). The water cycle in the closed chamber is shown in blue. **(b) Photograph**
128 **of the closed chamber used in the experiment with *Festuca arundinacea*.**
129
130 Seeds of *Festuca arundinacea (Schreb.)*, also commonly called tall fescue, were first sown in a
131 commercial potting soil (Terreau universel, Botanic, France. Composition: black and blond peat, wood
132 fibre, green compost and vermicompost manure, organic and organo-mineral fertilizers and
133 micronutrient fertilizers). During 15 to 20 days, they were then placed in a growth chamber of the
134 Microcosms experimental platform of the European Ecotron of Montpellier
135 (https://www.ecotron.cnrs.fr) under diurnal cycles of enlightenment, air temperature set at 20°C (T_{air}),
136 air relative humidity (RH) at 80 % and CO_2 atmospheric concentration close to ambient air
137 (concentration of CO_2 = 400 ppm).
138 Twelve pots (8 cm × 8 cm × 12 cm with 180 to 200 g of dry soil) containing approximatively 25 to 30
139 fescue mature plants were used for each experimental run. All plants were placed in a plastic tray filled
140 with tap water, inside an airtight transparent chamber manufactured from welded polycarbonate (10
141 mm wall thickness and 120 liters volume) similar to the chambers used by Milcu et al. (2013) (Fig. 1).
142 The sealing of the closed chamber was checked before each experiment using helium.

https://doi.org/10.5194/bg-2021-324
Preprint. Discussion started: 16 December 2021

To control temperature and light intensity inside the closed chamber, this one was placed in a larger controlled environment growth chamber. Light was provided by two plasma lamps (GAVITA Pro 300 LEP02; GAVITA) with PAR = 200 $\mu mol \cdot m^{-2} \cdot s^{-1}$ and air temperature inside the closed chamber was regulated at 19 ± 1 °C by adjusting the growth chamber temperature.

The closed chamber (Fig. 1) was used as a closed gas exchange system with controlled, and continuously monitored, environmental parameters. Air and soil temperature (CTN 35, Carel), air relative humidity (PFmini72, Michell instrument, USA) and CO_2 atmospheric concentration (GMP343, Vaisala, Finland) were measured and recorded using the growth chamber datalogger (sampling rate = 1 min). O_2 concentration was continuously monitored using an optical sensor (Oxy1-SMA, Presens, Germany).

Air relative humidity was regulated between 80 % and 90 % using a heat exchanger (acting as a condenser) connected to a closed cycle water cooling system. The condenser was positioned in a way to create a water closed cycle in the biological chamber (water vapor from evapotranspiration condense back into irrigation water). In order to keep the CO_2 mixing ratio close to 400ppm during the light periods, photosynthetic CO_2 uptake was compensated with injections of pure CO_2 using a mass flow controller (F200CV, Bronkhorst, The Netherlands). During the dark periods, a soda lime trap connected to a micro-pump (NMS 020B, KNF, Germany) was used to remove the excess CO_2 coming from respiration. CO_2 atmospheric concentration during the night was kept below 200 ppm.

To ensure atmospheric pressure stability in the closed chamber, a pressure compensation system, made of two connected 10 liters gas tight bags (multi-layers foil bags, Restek, USA), was installed. Each bag was half full of atmospheric air, the first one was installed in the closed chamber while the second one was outside this chamber. This way, each bag inflates or deflates in response to pressure variation either due to O_2 or CO_2, uptake or release. The pressure difference between the closed chamber and the atmosphere was regularly measured using a differential sensor (FD A602-S1KAlmemo, Ahlborn, Germany).

Finally, the enclosed air was mixed and considered homogeneous using seven brushless fans.

2.1.2. Gas sampling

To measure the isotopic composition along the experiment, small samples of gas were collected in 5 mL glass flasks, made of two Louwers H.V. glass valves (1-way bore 9mm Ref. LH10402008, Louwers Hanique, The Netherlands) welded together. Those flasks, previously evacuated, were mounted on PFA tubing ($1/4^{th}$) using two $1/4^{th}$ UltraTorr fitting (SS-4-UT-9, Swagelok, USA). Two manual valves (SS-4H, Swagelok, USA) were also installed on the PFA tubes to open or close the circuit. A micro-pump

https://doi.org/10.5194/bg-2021-324
Preprint. Discussion started: 16 December 2021

(NMS 20B, KNF, Germany) was finally turned on during air sampling to ensure closed chamber atmosphere circulation through the flask.

2.2. Isotopic measurements

2.2.1. Water extraction from leaf and isotopic analysis

After each experiment, the plant leaves were collected, placed in airtight flasks and immediately frozen at - 20°C for at least 24 hours to make sure there was minimal loss of water through vaporization when the vial was opened later. The extraction of water from leaves was done according to the procedure detailed in Alexandre et al. (2018). The vial was fixed onto a cryogenic extraction line and was first immerged in a liquid nitrogen Dewar to prevent any sublimation of the water. The water extraction line was emptied of most of its air (< 10^{-5} Pa). Once this pressure has been reached, the pump was turned off and a valve was closed in order to keep a constant static void within the system. The "reception" vial was then immerged in a liquid nitrogen Dewar (which will act as a water trap) and the sample vial was immerged in water maintained at 75°C. The system was kept in these conditions for no less than six hours, so that all the water present in the leaf and stems was extracted. Afterwards, in order to remove all of the organic compounds of the extracted water, an active charcoal was placed in the extracted water and left under agitation for the night.

For analysis of $\delta^{17}O$ and $\delta^{18}O$ of water, leaf water was converted to O_2 using a fluorination line for reaction of H_2O with CoF_3 heated to 370°C at LSCE. The isotopic composition of the dioxygen was measured by IRMS equipped with dual inlet (Thermo Scientific MAT253 mass spectrometer). The standard that was chosen was an O_2 standard calibrated against VSMOW. The precision was 0.015 ‰ for $\delta^{17}O$, 0.010 ‰ for $\delta^{18}O$ and 6 ppm for $\Delta^{17}O$ (for more details, refer to Landais et al. 2006).

2.2.2. O_2 purification and isotopic analysis

The air samples collected in the closed chambers were transported to LSCE for analyses of isotopic composition of O_2. The flasks were connected on a semi-automatic separation line inspired from Barkan and Luz (2003) which was made up of 8 ports in which 2 standards (outside air) and 6 samples were analyzed daily (Brandon et al., 2020). After pumping the whole line, the air was circulated through a water trap (ethanol at - 100°C) and then through a carbon dioxide trap immersed in liquid nitrogen at - 196°C. After collection of the gas samples on a molecular sieve trap cooled at - 196°C, a helium flow carried it through a chromatographic column which was immersed in a water reservoir at 0°C to

https://doi.org/10.5194/bg-2021-324
Preprint. Discussion started: 16 December 2021

separate the dioxygen and the argon from the dinitrogen. After separation of the dioxygen and argon from helium, the gas was collected in a stainless-steel manifold immersed in liquid helium at - 269°C.

After collection, the samples were analyzed by the IRMS previously mentioned for leaf water analyses. The following ratios were measured: $^{18}O/^{16}O$, $^{17}O/^{16}O$ and O_2/Ar (as an indicator of the O_2 concentration since Ar is an inert gas). $\delta^{17}O$ and $\delta^{18}O$ of each sample were obtained through 3 series of 24 dual inlet measurements against a standard made of O_2 and Ar. This sequence was followed by 2 peak jumping analyses of the O_2/Ar ratio including separate measurements of the O_2 and Ar signals for both the standard and the sample. The uncertainty associated with each measurement was obtained from the standard deviation of the three runs and from the repeated peak jumping measurement for $\delta O_2/Ar$. The uncertainty values for $\Delta^{17}O$, $\delta^{18}O$ and $\delta O_2/Ar$ were respectively 10 ppm, 0.05 ‰ and 0.5 ‰.

Each day, we performed measurements of the dioxygen isotopic composition and O_2/Ar ratio on two samples of outside air which is the standard for isotopic composition of O_2 (Hillaire-Marcel et al., 2021). So that the calibrated $\delta^{18}O$ value for our sample was calculated as in equation 2:

$$\delta^{18}O_{calibrated} = \left[\frac{(\delta^{18}O_{measured}/1000)+1}{(\delta^{18}O_{outsideair}/1000)+1} - 1\right] \times 1000 \quad (2)$$

2.3. Experimental runs

2.3.1. General strategy

Our goal was to calculate the fractionation factor associated with $\delta^{17}O$ and $\delta^{18}O$ for soil respiration, dark respiration and photosynthesis using the microcosm described above. In order to quantify the fractionation factors, we needed to work in closed and controlled conditions. Given the volume of the closed chamber (120 L, hence about 1.12 moles of O_2) and the order of magnitude of dark respiration (order of magnitude of 0.08 μmol O_2 s^{-1} for soil respiration) and net photosynthetic fluxes (order of magnitude of 0.45 μmol O_2 s^{-1}) inside the chamber, we calculated that experiments should last from 23 days to more than 2 weeks so that more than one tenth of the O_2 in the chamber can be recycled by the plant and soil. This recycling allows the creation of sufficiently large isotopic signals (especially $\Delta^{17}O$ of O_2) to be detected and measured. We set up two different experiments in the closed chamber, each experiment being repeated 3 or 4 times to address experimental repeatability of the system.

https://doi.org/10.5194/bg-2021-324
Preprint. Discussion started: 16 December 2021

The first experiment (repeated 4 times, i.e. in 4 sequences) aimed at studying the fractionation coefficients during soil respiration. The second experiment (repeated 3 times, i.e. in 3 sequences, each sequence being divided into several periods with or without light) aimed at studying the fractionation coefficients during dark respiration and photosynthesis of plants.

Prior to the aforementioned experiments, measurements were carried out on a closed empty chamber to check the absence of leaks as well as the absence of isotopic fractionation (Table S1).

2.3.2. Soil respiration experiment

To conduct the soil respiration experiment, 2.6 kg of soil (*Terreau universel, Botanic*) were placed in 12 different pots. The light was turned off during this experimental run. During this dark period, CO_2 from soil respiration accumulates in the biological closed chamber. To have a stable concentration of CO_2 during the whole dark period, the CO_2 was trapped using soda lime. Four sequences were performed with respective durations of 53, 51, 43 and 36 days.

2.3.3. Photosynthesis and dark respiration experiment

We used the same soil with plants (*Festuca arundinacea)* grown before the start of the three sequences of the photosynthesis and dark respiration experiment. In order to obtain a significant change of the $\Delta^{17}O$ of O_2 signal in our closed 120 L chambers, the 3 experiments were run during 1 to 2 months. CO_2 level was controlled by a CO_2 trap and CO_2 injections. This was done to ensure that the CO_2 in the chamber did not reach levels too far from the atmospheric composition. This could have affected the physiology of the plant. The enlightenment was controlled to alternate between day (photosynthesis and respiration) and night conditions (respiration).

2.4. Quantification of fractionation coefficients

We detail below how we used the results from our experiments to quantify the associated fractionation coefficients. Notations used below are gathered in Table 1.

The isotopic fractionation coefficient of oxygen is expressed through the fractionation coefficient α.

$$^{18}\alpha = \frac{R^{18}O_{product}}{R^{18}O_{substrat}} \quad (3)$$

https://doi.org/10.5194/bg-2021-324
Preprint. Discussion started: 16 December 2021

where α is the fractionation coefficient and $R^{18}O$ is the ratio of the concentration $R^{18}O = \frac{n(^{18}O)}{n(^{16}O)}$ with n the number of moles of O_2 containing ^{18}O or ^{16}O. $R^{18}O$ is linked to the $\delta^{18}O$ value through:

$$\delta^{18}O = \left(\frac{R^{18}O_{sample}}{R^{18}O_{standard}} - 1\right) \times 1000 \quad (4)$$

The isotopic discrimination is related to the isotopic fractionation coefficient through:

$$^{18}\varepsilon = {}^{18}\alpha - 1 \quad (5)$$

The same equations (3), (4) and (5) can be proposed for $\delta^{17}O$ and the relationship between the fractionation coefficients $^{17}\varepsilon$ and $^{18}\varepsilon$ is written as:

$$\gamma = \frac{\ln {}^{17}\alpha}{\ln {}^{18}\alpha} \quad (6)$$

2.4.1. Soil respiration

Respiration is associated with isotopic fractionation. The light isotopes, ^{16}O, are more easily integrated by microorganisms than the heavy isotopes, ^{18}O, which hence remain in the atmosphere. We express the fractionation coefficient for soil respiration as:

$$^{18}\alpha_{soil\_respi} = \frac{R^{18}O_{breathed}}{R^{18}O_{air}} \quad (7)$$

In our experiment, the respiratory process took place in a closed reservoir so that we could calculate the fractionation coefficients from the evolution of the concentration and isotopic composition of dioxygen in the chamber. The evolution of the number of molecules of dioxygen in the air of the closed chamber, $n(O_2)$, between time t and time t+dt can be written as:

$$n(O_2)_t = n(O_2)_{t+dt} + dn(O_2) \quad (8)$$

with dn the number of dioxygen molecules respired during the time period dt. A similar equation can be written for the number of dioxygen molecules containing ^{18}O remaining in the air of the chamber:

$$R^{18}O_t \times n(O_2)_t = R^{18}O_{t+dt} \times n(O_2)_{t+dt} + R^{18}O_{t+dt} \times {}^{18}\alpha_{soil\_respi} \times dn(O_2) \quad (9)$$

https://doi.org/10.5194/bg-2021-324
Preprint. Discussion started: 16 December 2021

297 Combining equations Eq. (8) and Eq. (9) and integrating from t_0 (starting time of the experiment when
298 the chamber is closed) to t leads to:
299

300 $$^{18}\varepsilon_{soil\_respi} = {}^{18}\alpha_{soil\_respi} - 1 = \frac{ln\left(\frac{\frac{R^{18}O_t}{1000}+1}{\frac{R^{18}O_{t0}}{1000}+1}\right)}{\ln\left(\frac{n(O_2)_t}{n(O_2)_{t0}}\right)}$$

301 (10)
302

303 Since argon is an inert gas, we can link $\frac{n(O_2)_t}{n(O_2)_{t0}}$ to $\delta\left(\frac{O_2}{Ar}\right)$, so that:
304

305 $$\frac{n(O_2)_t}{n(O_2)_{t0}} = \frac{\frac{\delta\left(\frac{O_2}{Ar}\right)_t}{1000}+1}{\frac{\delta\left(\frac{O_2}{Ar}\right)_{t0}}{1000}+1} \quad (11)$$

306
307

308 **2.4.2. Dark respiration**

309 In order to calculate the fractionation associated with soil and plant respiration during dark period, we
310 followed the same calculation as for the soil respiration (section 2.4.1). In this case, we selected only
311 night periods from each sequence of the photosynthesis and dark respiration experiment.

312

313 **2.4.3. Photosynthesis**

314 During photosynthesis, the oxygen atoms in the dioxygen produced by the plant comes from the
315 oxygen atom of water consumed by photosynthesis in the leaves so that the fractionation coefficient
316 during photosynthesis can be expressed as:
317

318 $$^{18}\alpha_{photosynthesis} = \frac{R^{18}O_{\,produced\,O_2}}{R^{18}O_{lw}} \quad (12)$$

319

320 where *lw* stands for leaf water.
321

322 Photosynthesis occurs during the light periods. However, it should be noted that dark respiration,
323 photorespiration and Mehler's reaction (Mehler, 1951) occur at the same time. Thus, at each stage,

https://doi.org/10.5194/bg-2021-324
Preprint. Discussion started: 16 December 2021

dioxygen is both produced by photosynthesis and consumed by the aforementioned O_2 uptake processes (hereafter $total\_respi$) by the plant according to the mass conservation equation:

$$n(O_2)_t = n(O_2)_{t+dt} + dn_{total\_respi} + dn_{photosynthesis} \quad (13)$$

where dn_{total_respi} is the number of molecules of O_2 consumed by dark respiration, photorespiration and Mehler's reaction between time t and t+dt, and $dn_{photosynthesis}$ is the number of molecules of O_2 produced by photosynthesis between t and t+dt.

The budget for ^{18}O of O_2 can be written as:

$$R^{18}O_t \times \frac{n(O_2)_t}{n(O_2)_{t0}} = R^{18}O_{t+dt} \times \frac{n(O_2)_{t+dt}}{n(O_2)_{t0}} + R^{18}O_{t+dt} \times {}^{18}\alpha_{total\_respi} \times \frac{dn_{total\_respi}}{n(O_2)_{t0}} + R^{18}O_{lw} \times {}^{18}\alpha_{photosynthesis} \times \frac{dn_{photosynthesis}}{n(O_2)_{t0}} \quad (14)$$

where ${}^{18}\alpha_{total\_respi}$ is the fractionation coefficients associated with each O_2 consuming process periods throughout the whole experiment.

We introduced the normalized fluxes of photosynthesis and total respiration as:

$$F_{photosynthesis} = \left|\frac{dn_{photosynthesis}}{n(O_2)_{t0} \times dt}\right| \quad (15)$$

$$F_{total\_respi} = \left|\frac{dn_{total\_respi}}{n(O_2)_{t0} \times dt}\right| \quad (16)$$

$$aR^{18} = \left|\frac{dR^{18}O}{dt}\right| \quad (17)$$

This led to the following expression of ${}^{18}\alpha_{photosynthesis}$:

$${}^{18}\alpha_{photosynthesis} = \frac{-aR^{18} + F_{photosynthesis} - F_{total\_respi} + {}^{18}\alpha_{total\_respi} \times F_{total\_respi}}{R^{18}O_{lw} \times F_{photosynthesis}} \quad (18)$$

${}^{18}\alpha_{photosynthesis}$ depends on the values of ${}^{18}\alpha_{total\_respi}$ and of F_{total_respi}, themselves dependent on the values of ${}^{18}\alpha_{Mehler}$ (fractionation factor associated with Mehler reaction), F_{Mehler} (flux of

https://doi.org/10.5194/bg-2021-324
Preprint. Discussion started: 16 December 2021

355 oxygen related to Mehler reaction), ${}^{18}\alpha_{dark\_respi}$, F_{dark_respi}, ${}^{18}\alpha_{photorespi}$ (fractionation factor
356 associated with photorespiration) and $F_{photorespi}$ (photorespiration flux of oxygen). These last 4
357 parameters could not be determined in our global experiment. Our determination of ${}^{18}\alpha_{photosynthesis}$
358 will thus rely on assumptions for the estimations of ${}^{18}\alpha_{Mehler}$, F_{Mehler}, ${}^{18}\alpha_{photorespi}$ and $F_{photorespi}$.
359
360 To separate the ${}^{18}\alpha_{dark\_respi}$ from the other fractionation factors, we defined:
361
362 $${}^{18}\alpha_{total\_respi} = {}^{18}\alpha_{photorespi} \times f_{photorespi} + {}^{18}\alpha_{Mehler} \times f_{Mehler} + {}^{18}\alpha_{dark\_respi} \times f_{dark\_respi}$$
363 (19)
364 with
365
366 $$F_{total\_respi} = F_{dark\_respi} + F_{photorespi} + F_{Mehler} \quad (20)$$
367
368
369 f indicates the fraction of the total oxygen uptake flux corresponding to each process (dark
370 respiration, photorespiration and Mehler's reaction) so that:
371
372 $$f_{dark\_respi} + f_{photorespi} + f_{Mehler} = 1 \quad (21)$$
373
374 $$F_{dark\_respi} = f_{dark\_respi} \times F_{total\_respi} \quad (22)$$
375
376 $$F_{photorespi} = f_{photorespi} \times F_{total\_respi} \quad (23)$$
377
378 $$F_{Mehler} = f_{Mehler} \times F_{total\_respi} \quad (24)$$
379
380 In the absence of further constraints, we used here as first approximation the global values from
381 Landais et al. (2007) for f_{dark_respi} (0.6), $f_{photorespi}$ (0.3) and f_{Mehler} (0.1). Values for $\alpha_{photorespi}$ and
382 α_{Mehler} were based on the most recent estimates of Helman et al. (2005).
383
384 **Table 1. List of variables used to quantify fractionations.** * means either oxygen 17 or oxygen 18.

Symbol	Description
${}^{*}\alpha$	Fractionation coefficient

https://doi.org/10.5194/bg-2021-324
Preprint. Discussion started: 16 December 2021

${}^{*}\alpha_{dark\_respi}$	Fractionation coefficient of soil and plant respiration during night periods
${}^{*}\alpha_{dark\_leave\_respi}$	Fractionation coefficient of respiration of leave during night periods
${}^{*}\alpha_{Mehler}$	Fractionation coefficient associated with Mehler respiration
${}^{*}\alpha_{photorespi}$	Fractionation coefficient associated with photorespiration
${}^{*}\alpha_{photosynthesis}$	Fractionation coefficient associated with photosynthesis
${}^{*}\alpha_{soil\_respi}$	Fractionation coefficient associated with soil respiration
${}^{*}\alpha_{total\_respi}$	Fractionation coefficient associated with total respiration during light period
${}^{*}\varepsilon$	Isotopic discrimination
${}^{*}\varepsilon_{dark\_respi}$	Isotopic discrimination of soil and plant respiration during night periods
${}^{*}\varepsilon_{dark\_leave\_respi}$	Isotopic discrimination of respiration of leave during night periods
${}^{*}\varepsilon_{photosynthesis}$	Isotopic discrimination associated with photosynthesis
${}^{*}\varepsilon_{soil\_respi}$	Isotopic discrimination of soil respiration associated with soil respiration experiment
γ	Ratio of $ln({}^{17}\alpha)\ to\ ln({}^{18}\alpha)$
γ_{dark_respi}	Ratio of $ln({}^{17}\alpha_{dark\_respi})\ to\ ln({}^{18}\alpha_{dark\_respi})$
$\gamma_{dark\_leave\_respi}$	Ratio of $ln({}^{17}\alpha_{dark\_leave\_respi})\ to\ ln({}^{18}\alpha_{dark\_leave\_respi})$
$\gamma_{photosynthesis}$	Ratio of $ln({}^{17}\alpha_{photosynthesis})\ to\ ln({}^{18}\alpha_{photosynthesis})$
γ_{soil_respi}	Ratio of $ln({}^{17}\alpha_{soil\_respi})\ to\ ln({}^{18}\alpha_{soil\_respi})$

https://doi.org/10.5194/bg-2021-324
Preprint. Discussion started: 16 December 2021

aN	Linear regression coefficient of the evolution of $n(O_2)$ as a function of time
aR	Linear regression coefficient of the evolution of R^*O as a function of time
$dn_{photosynthesis}$	Number of molecules of O_2 produced by photosynthesis between t and t+dt
dn_{total_respi}	Number of molecules of O_2 consumed by total respiration during light periods between time t and t+dt
F_{dark_respi}	Dark respiration flux (normalized vs number of O_2 molecules at the start of the experiment)
F_{Mehler}	Mehler flux (normalized vs number of O_2 molecules at the start of the experiment)
$F_{photorespi}$	Photorespiration O_2 flux (normalized vs number of O_2 molecules at the start of the experiment)
$F_{photosynthesis}$	Photosynthesis O_2 flux (normalized vs number of O_2 molecules at the start of the experiment)
F_{total_respi}	Total respiration O_2 flux during light period (normalized vs number of O_2 molecules at the start of the experiment)
f_{dark_respi}	Fraction of the dioxygen flux corresponding to dark respiration process
f_{Mehler}	Fraction of the dioxygen flux corresponding to Mehler process
$f_{photorespi}$	Fraction of the dioxygen flux corresponding to photorespiration process
$n(O_2)$	Number of moles of O_2
R^*O	Ratio of heavy (^{18}O or ^{17}O) isotope to light isotope (^{16}O)
R^*O_{lw}	R^*O of leaf water

3.Results

3.1. Soil Respiration

3.1.1. Experimental data

https://doi.org/10.5194/bg-2021-324
Preprint. Discussion started: 16 December 2021

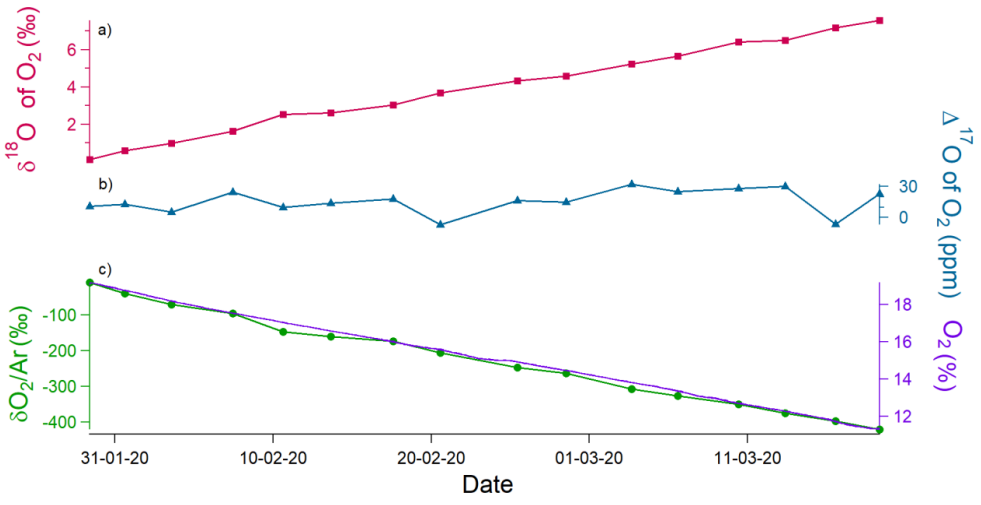

Fig.2. Evolution of the different concentrations and isotopic ratios in the sequence 2 of the soil respiration experiment. (a) $\delta^{18}O$ of O_2 (red) variations. (b) $\Delta^{17}O$ of O_2 (blue) variations. (c) Dioxygen concentration (purple) and $\delta O_2/Ar$ variations (green).

During the 4 sequences, the respiration activity led to a decreasing level of the O_2 concentration measured by the optical sensor or through the $\delta O_2/Ar$ evolution from IRMS measurements (Fig. S1). The comparison of the evolution of the O_2 concentration during the different sequences showed that respiratory fluxes were different with a maximum factor of 4 between the different sequences (Fig. S1). In parallel to the decrease in O_2 concentration, the $\delta^{18}O$ increased as expected since respiration preferentially consumes the lightest isotopes: over the 51 days of the 2nd soil respiration sequence, we observed a linear decrease of oxygen concentration by more than 5% while $\delta^{18}O$ increased by 8 ‰ (Fig. 2). A Mann-Kendall test (95%) showed that the $\Delta^{17}O$ of O_2 does not show any trend within 95% over the 4 sequences (Fig. S2).

3.1.2. Fractionation coefficients

We used the 15 to 20 samples obtained during each sequence of soil respiration experiment to draw the relative evolution of $ln(R^{18}O_t/R^{18}O_{t0})$ vs $ln\left((\delta\left(\frac{O_2}{Ar}\right)_t/1000+1)/(\delta\left(\frac{O_2}{Ar}\right)_{t0}/1000+1)\right)$ following Eq. (10) (Fig. 3). The slope of the corresponding regression line provided the isotopic discrimination ${}^{18}\varepsilon_{soil\_respi}$ and hence the fractionation coefficient ${}^{18}\alpha_{soil\_respi}$ for each sequence. (Table S2). It could be observed that despite differences in respiratory fluxes for the different

https://doi.org/10.5194/bg-2021-324
Preprint. Discussion started: 16 December 2021

410 sequences, the relationship between $\delta^{18}O$ of O_2 and O_2 concentration (or $\delta O_2/Ar$) and hence the
411 calculated fractionation factor associated with respiration is not much affected. The observed
412 differences between respiratory fluxes could be explained by the small variations in organic carbon
413 and by a different development of microbial populations during the different experiments.

414

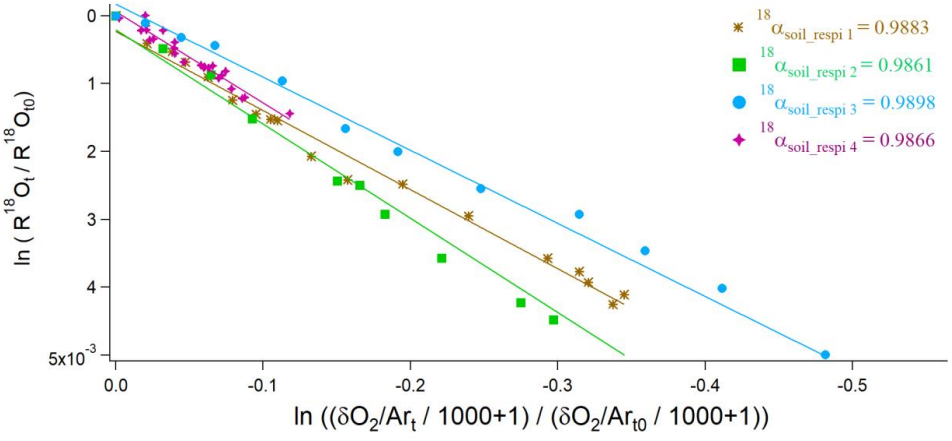

415

416 **Fig.3 Determination of $^{18}O/^{16}O$ fractionation coefficients in the 4 respiration sequences.**
417 **$^{18}\alpha_{soil\_respi\ 1}$ (brown), $^{18}\alpha_{soil\_respi\ 2}$ (green), $^{18}\alpha_{soil\_respi\ 3}$ (blue), $^{18}\alpha_{soil\_respi\ 4}$ (purple) are**
418 **respectively respiratory fractionation coefficients associated with sequences 1 to 4.**

419 Using the results of the 4 sequences, we determined the values for the mean isotopic discrimination
420 $^{18}\varepsilon_{soil\_respi}$ (- 12.3 ± 1.7 ‰), the mean isotopic discrimination $^{17}\varepsilon_{soil\_respi}$ (- 6.4 ± 0.9 ‰) and the
421 average γ_{soil_respi} (0.5164 ± 0.0005).

422

423 **3.2. Photosynthesis and dark respiration**

424 **3.2.1. Experimental data**

https://doi.org/10.5194/bg-2021-324
Preprint. Discussion started: 16 December 2021

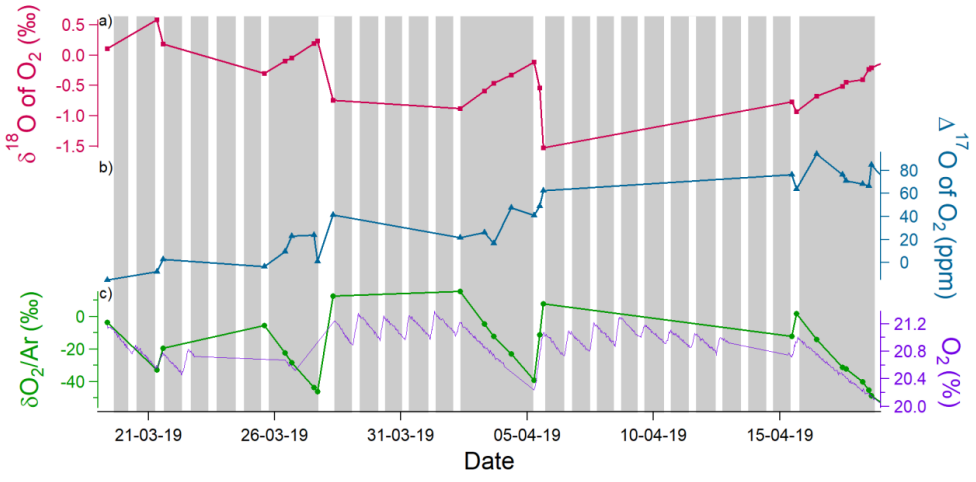

Fig.4. Example of the evolution of the different concentrations and isotopic ratios in the sequence 1 of photosynthesis and dark respiration experiment in the closed chamber over 30 days. Grey rectangles correspond to night periods and white rectangles to light periods. (a) $\delta^{18}O$ of O_2 (red) variations. (b) $\Delta^{17}O$ of O_2 variations (blue) and regulation of carbon dioxide flux (purple). (c) Dioxygen concentration (purple) and $\delta O_2/Ar$ variations (green).

During the night periods, when only respiration occurred, we observed a decrease in O_2 concentration by 1% within 3 days and a $\delta^{18}O$ increase by 1 ‰ during the same period (Fig. 4). The evolution was qualitatively similar with that of soil respiration experiments with higher fluxes. We observed the same trends for the evolution of $\delta O_2/Ar$ during the night periods as for the respiration experiment. During light periods, there was a marked decrease in $\delta^{18}O$ (2 ‰) and a marked increase in the flow of oxygen released (1%) during 1 day. This result was consistent with previous studies of Guy et al. (1993) and Eisenstadt et al. (2010) showing that photosynthesis produces oxygen with the $\delta^{18}O$ value close to the $\delta^{18}O$ of the leaf water, leaf water $\delta^{18}O$ being lower than atmospheric $\delta^{18}O$ of O_2. We observed the same trends for the evolution of $\delta O_2/Ar$ during the night periods as for the respiration experiment.

The Mann-Kendall test (95%) showed a significative increasing trend of the $\Delta^{17}O$ of O_2 over sequences 1 and 2 (Fig. S3) ($\simeq$ 100 ppm in 30 days for sequence 1, $\simeq$ 100 ppm in 40 days for sequence 2) while no significant increase of $\Delta^{17}O$ of O_2 is observed over sequence 3 (Fig. S3).

3.2.2. Fractionation coefficients

Dark respiration

https://doi.org/10.5194/bg-2021-324
Preprint. Discussion started: 16 December 2021

The average of the isotopic discrimination for dark respiration ${}^{18}\varepsilon_{dark\_respi}$ and ${}^{17}\varepsilon_{dark\_respi}$ were calculated over the 9 night periods and we obtained values of respectively - 17.0 ± 2.0 ‰ and - 8.5 ± 0.8 ‰. The average of γ_{dark_respi} during the experiment was equal to 0.5124 ± 0.0084 (Table S3).

The dark respiration of this experiment includes respiration of both soil and leave. Because soil respiration fractionation coefficient has been determined above, it is possible to estimate here the fractionation coefficient for the dark leave respiration:

$$F_{dark\_respi} = F_{soil\_respi} + F_{dark\_leave\_respi} \quad (25)$$

$${}^{18}\alpha_{dark\_respi} = f_{soil\_respi} \times {}^{18}\alpha_{soil\_respi} + f_{dark\_leave\_respi} \times {}^{18}\alpha_{dark\_leave\_respi} \quad (26)$$

with $F_{dark\_leave\_respi}$ the flux of leave respiration during the night, f_{soil_respi} the fraction of soil respiration during night periods (F_{soil_respi} / F_{dark_respi}) and $f_{dark\_leave\_respi}$ the fraction of dark leave respiration during night periods ($F_{dark\_leave\_respi}$ / F_{dark_respi}).

$${}^{18}\alpha_{dark\_leave\_respi} = \frac{{}^{18}\alpha_{dark\_respi} - f_{soil\_respi} \times {}^{18}\alpha_{soil\_respi}}{f_{dark\_leave\_respi}} \quad (27)$$

The isotopic discriminations ${}^{18}\varepsilon_{dark\_leave\_respi}$ and ${}^{17}\varepsilon_{dark\_leave\_respi}$ were respectively equals to - 19.1 ± 2.4 ‰ and - 9.7 ± 0.9 ‰. The average of the gamma value was equal to 0.5089 ± 0.0777. The standard deviations (1 σ) was calculated by a Monte Carlo method from the individual uncertainties of the ${}^{18}\alpha_{dark\_respi}$, ${}^{18}\alpha_{soil\_respi}$, F_{soil_respi} and F_{dark_respi}.

Photosynthesis

In order to calculate an average value for fractionation coefficient associated with photosynthesis from Eq. (18), we first calculated the averages of the flux of the O_2 consuming processes and of the fractionation coefficients associated with each sequence: $\langle F_{total\_respi} \rangle$ and $\langle {}^{18}\alpha_{total\_respi} \rangle$. We also calculated the net O_2 flux during light periods, $aN = F_{photosynthesis} - F_{total\_respi}$, as the linear regression, aN, of $\frac{n(O_2)_t}{n(O_2)_{t0}}$ with time. aR^{18} is also obtained as a linear regression of $R^{18}O$ with time over each light period. Our data support our assumption that the regime was stationary over time, i.e.

https://doi.org/10.5194/bg-2021-324
Preprint. Discussion started: 16 December 2021

that $R^{18}O$ and $n(O_2)_t / n(O_2)_{t0}$ evolved linearly over time, which is why we were able to do linear regressions.

$$^{18}\alpha_{photosynthesis} = \frac{-\ aR^{18} + aN + \langle ^{18}\alpha_{total\_respi}\rangle \times \langle F_{total\_respi}\rangle}{R^{18}O_{lw} \times F_{photosynthesis}} \quad (28)$$

We finally estimated the values of $^{18}\varepsilon_{photosynthesis}$ and $^{17}\varepsilon_{photosynthesis}$ as 3.7 ± 1.3 ‰ and 1.9 ± 0.6 ‰, respectively. The average of the gamma value was equal to 0.5207 ± 0.0537, a value which depends on the value taken for the $\delta^{18}O$ value of atmospheric air vs VSMOW (Sharp and Wostbrock, 2021), see Table 2. Sensitivity tests (Tables S4, S5 and S6) on values of the O_2 flux and associated fractionation coefficients for photorespiration and Mehler reaction resulted in uncertainty estimates of 0.0012 and 0.0007 for the values of $^{18}\alpha_{photosynthesis}$ and $^{17}\alpha_{photosynthesis}$ (Table S6).

The value of isotopic fractionation associated with the light period of period 1 of sequence 1 appeared clearly out of range. Following the Dixon's outlier detection test (Dixon, 1960), this value was considered an anomaly (likelihood > 99 %) and was removed from further analysis (Table S7). The individual determination is presented on Table S7.

4.Discussion

4.1. $\Delta^{17}O$ of O_2

The $\Delta^{17}O$ of O_2 is equal to 0 by definition for atmospheric air, and hence it should be equal to zero at the beginning of each experiment. The observed change during an experiment can only be driven by biological processes since the interaction with stratosphere is not possible in the closed chambers.

During the soil respiration experimental run, the $\Delta^{17}O$ of O_2 was constant. This directly reflects the γ_{soil_respi} value of 0.5164 ± 0.0005 found for respiration (Table 2) since $\Delta^{17}O$ of O_2 is defined with a slope of 0.516 between $\ln(1+\delta^{17}O)$ and $\ln(1+\delta^{18}O)$ (Eq. 1). This result is in good agreement and within the uncertainties given by Helman et al. (2005) with the γ value of 0.5174 ± 0.0003 obtained with respiration experiments on several micro-organisms.

During the experiment involving both oxygen uptake and photosynthesis, the $\Delta^{17}O$ of O_2 has a globally increasing trend with values reaching about 100 ppm after one month. Such behavior is expected and was already observed by Luz et al. (1999) with $\Delta^{17}O$ of O_2 values reaching 150 ppm after a 200-day experiment within a closed terrarium. This increase cannot be explained by respiration since respiration does not modify $\Delta^{17}O$ of O_2. It is hence mainly due to photosynthesis producing oxygen

https://doi.org/10.5194/bg-2021-324
Preprint. Discussion started: 16 December 2021

with a $\Delta^{17}O$ of O_2 different from the atmospheric one. Previous analyses have shown that the $\Delta^{17}O$ of H_2O of VSMOW (close to mean oceanic water) expressed vs isotopic composition of atmospheric O_2 has a value between 134 to 223 ppm (using a definition of $\Delta^{17}O$ of $H_2O = \ln(1+\delta^{17}O) - 0.516 \times \ln(1+\delta^{18}O)$) (Sharp and Wostbrock, 2021). Within the water cycle, the slopes of $\ln(1+\delta^{17}O)$ vs $\ln(1+\delta^{18}O)$ for the meteoric line, evaporation and evapotranspiration lines are larger than 0.516 (Li and Meijer, 1998; Landais et al., 2006) so that $\Delta^{17}O$ of water consumed by the plants during photosynthesis should be slightly lower than the $\Delta^{17}O$ of VSMOW expressed vs isotopic composition of atmospheric O_2 but still higher than the $\Delta^{17}O$ of atmospheric O_2. The photosynthesis is thus responsible for the $\Delta^{17}O$ of O_2 increase in the closed chamber.

4.2. Fractionation factors associated with $\delta^{18}O$ of O_2 and implications for the Dole effect

Table 2. Summary of the mean values of the isotopic discriminations and gamma values of all sequences of (1) the soil respiration experiment and of (2) the respiration and photosynthesis experiment and the number of data on which they were calculated. ** is the value for $\gamma_{photosynthesis}$ that depends on the determination of the $\delta^{17}O$ of atmospheric O_2 vs $\delta^{17}O$ of VSMOW. We provide here the two different possible estimates using either 12.03 ‰ (Luz and Barkan, 2011) or 12.08 ‰ (Barkan and Luz, 2005): value determined with $\delta^{17}O$= 12.03 ‰ / value determined with $\delta^{17}O$ = 12.08 ‰.

	Average (‰)	Standard deviation (‰)	Number of data
$^{18}\varepsilon_{soil\_respi}$	-12.3	1.7	4
$^{17}\varepsilon_{soil\_respi}$	-6.4	0.9	4
γ_{soil_respi}	0.5164	0.0005	4
$^{18}\varepsilon_{dark\_respi}$	-17.0	2.0	9
$^{17}\varepsilon_{dark\_respi}$	-8.5	0.8	9
γ_{dark_respi}	0.5124	0.0084	9
$^{18}\alpha_{dark\_leave\_respi}$	-19.1	2.4	9
$^{17}\alpha_{dark\_leave\_respi}$	-9.7	0.9	9
$\gamma_{dark\_leave\_respi}$	0.5089	0.0777	9
$^{18}\varepsilon_{photosynthesis}$	3.7	1.3	8
$^{17}\varepsilon_{photosynthesis}$	1.9	0.6	8
$\gamma_{photosynthesis}$	0.5207/0.5051**	0.0537/0.0504**	8

https://doi.org/10.5194/bg-2021-324
Preprint. Discussion started: 16 December 2021

The isotopic discrimination $^{18}\varepsilon_{soil\_respi}$ = - 12.3 ± 1.7‰ for the soil respiration experiments is comparable to the average terrestrial soil respiration fractionation found by Angert et al. (2001) of - 12‰. Still, among the diversity of soils studied by Angert et al. (2001), the soils showing the $^{18}\varepsilon$ values closest to our values are clay soil ($^{18}\varepsilon$ = - 13‰) and sandy soil ($^{18}\varepsilon$ = - 11‰). These soils are different from our soil which was enriched in organic matter. Further experiments are then needed to understand the variability in $^{18}\varepsilon$ associated with soil respiration.

The isotopic discrimination for dark respiration in leave, $^{18}\varepsilon_{dark\_leave\_respi}$ = - 19.1 ± 2.4 ‰ is associated with a large uncertainty and would benefit from additional experiments with a higher sampling and measurement rate. Still, even if it was obtained on different organism and experimental set-up, this value is in agreement with the values for isotopic discrimination for dark respiration determined by Helman et al. (2005) on bacteria from the Lake Kinneret ($^{18}\varepsilon$ = -17.1 ‰) and Synechocystis ($^{18}\varepsilon$ = - 19.4 ‰ and - 19.5 ‰).

The average $^{18}\varepsilon_{photosynthesis}$ is + 3.7 ± 1.3‰ which goes against the classical assumption that terrestrial photosynthesis does not fractionate (Guy et al., 1993). This value for the isotopic discrimination is smaller than the photosynthetic fractionation in marine environment $^{18}\varepsilon$ = + 6 ‰ found by Eisenstadt et al. (2010). Still, this result suggests that the terrestrial Dole effect may be higher than currently assumed and challenge the assumption that terrestrial and oceanic Dole effects have the same values (Luz and Barkan, 2011).

4-Conclusion

Using a simplified analog of the terrestrial biosphere in a closed chamber we found that the fractionation factors of soil respiration and dark respiration of leave at the chamber level agree with the previous estimates derived from studies at micro-organism level. This is an important confirmatory step for the fractionation factors previously used to estimate the global Dole effect. More importantly, we document for the first time a significant ^{18}O fractionation during terrestrial photosynthesis (+ 3.7 ‰ ± 1.3‰). If confirmed by future studies, this can have a substantial impact on the calculation of the Dole effect, with important consequences for our estimates of the past global primary production.

Our study showed the usefulness of closed chamber to quantify the fractionation factors associated with biological processes in the oxygen cycle at the plant level. The main limitation of our present study was the low sampling rate during our experiments which hamper the precision of the determined fractionation factors. Future work should use this validated set-up to multiply such experiments to

https://doi.org/10.5194/bg-2021-324
Preprint. Discussion started: 16 December 2021

improve the precision of fractionation factors and to explore the variability of fractionation factors for different plants and hence different metabolisms. A good application would be to study the difference between C3 and C4 plants because C4 plants do not photorespiration.

Data availability

All individual fractionation coefficients for each experiment are given in the Supplement.

Author contributions

AL and CPi designed the project. CPi, JS and SD carried out experiments at ECOTRON of Montpellier and FP, CPa, RJ, AD and OJ at LSCE. CPa, NP and AL analyzed the data. CPa and AL prepared the manuscript with contributions from NP, CPi, JS and AM.

Competing interests

The authors declare that they have no conflict of interest.

Acknowledgements

The research leading to these results has received funding from the European Research Council under the European Union H2020 Programme (H2020/20192024)/ERC grant agreement no. 817493 (ERC ICORDA) and ANR HUMI17. The authors acknowledge the scientific and technical support of PANOPLY (Plateforme ANalytique géOsciences Paris-sacLaY), Paris-Saclay University, France. We would also like to thank Abdelaziz Faez and Olivier Ravel from ECOTRON of Montpellier for their help, and Anne Alexandre from CEREGE at Aix-en-Provence.

References

Alexandre, A., Landais, A., Vallet-Coulomb, C., Piel, C., Devidal, S., Pauchet, S., Sonzogni, C., Couapel, M., Pasturel, M., Cornuault, P., Xin, J., Mazur, J-C., Prié, F., Bentaleb, I., Webb, E., Chalié, F., and Roy, J.: The triple oxygen isotope composition of phytoliths as a proxy of continental atmospheric humidity: insights from climate chamber and climate transect calibrations, Biogeosciences, 15,

584 3223-3241, https://doi.org/10.5194/bg-15-3223-2018, 2018.
585
586 Angert, A., Luz, B., and Yakir, D.: Fractionation of oxygen isotopes by respiration and diffusion in
587 soils and its implications for the isotopic composition of atmospheric O_2, Global Biogeochem. Cy.,
588 15, 871-880, https://doi.org/10.1029/2000GB001371, 2001.
589
590 Angert, A., Barkan, E., Barnett, B., Brugnoli, E., Davidson, E. A., Fessenden, J., Maneepong, S.,
591 Panapitukkul,N., Randerson, J. T., Savage, K., Yakir, D., and Luz, B.: Contribution of soil respiration in
592 tropical, temperate, and boreal forests to the ^{18}O enrichment of atmospheric O_2, Global
593 Biogeochem. Cy., 17, 1089, https://doi.org/10.1029/2003GB002056, 2003.
594
595 Barkan, E., and Luz, B.: High precision measurements of $^{17}O/^{16}O$ and $^{18}O/^{16}O$ of O2 and O2/Ar ratio in
596 air, Rapid Commun. Mass Spectrom., 17, 2809-2814, https://doi.org/10.1002/rcm.1267, 2003.
597
598 Barkan, E., and Luz, B.: High precision measurements of $^{17}O/^{16}O$ and $^{18}O/^{16}O$ ratios in H_2O, Rapid
599 Commun. Mass Spectrom., 19, 3737-3742, https://doi.org/10.1002/rcm.2250, 2005.
600
601 Bender, M., Sowers, T., Dickson, M-L., Orchardo, J., Grootes, P., Mayewski, P. A., and Meese, D. A.:
602 Climate correlations between Greenland and Antarctica during the past 100,000 years, Nature, 372,
603 663-666, https://doi.org/10.1038/372663a0, 1994.
604
605 Blunier, T., Barnett, B., Bender, M. L., and Hendricks, M. B.: Biological oxygen productivity during the
606 last 60,000 years from triple oxygen isotope measurements, Global Biogeochem. Cy., 16, 3-4,
607 https://doi.org/10.1029/2001GB001460, 2002.
608
609 Brandon, M., Landais, A., Duchamp-Alphonse, S., Favre, V., Schmitz, L., Abrial, H., Prié, F., Extier, T.,
610 and Blunier, T.: Exceptionally high biosphere productivity at the beginning of Marine Isotopic Stage
611 11, Nat. Commun., 11, 1-10, https://doi.org/10.1038/s41467-020-15739-2, 2020.
612
613 Dixon, W. J.: Simplified estimation from censored normal sample, Ann. Math. Stat., 21, 488-506,
614 https://doi.org/10.1214%2Faoms%2F1177729747, 1960.
615
616 Dole, M., Lane, G. A., Rudd, D. P., and Zaukelies, D. A.: Isotopic composition of atmospheric oxygen
617 and nitrogen, Geochim. Cosmochim. Ac., 6, 65-78, https://doi.org/10.1016/0016-7037(54)90016-2,

https://doi.org/10.5194/bg-2021-324
Preprint. Discussion started: 16 December 2021

618 1954.
619
620 Dreyfus, G. B., Parrenin, F., Lemieux-Dudon, B., Durand, G., Masson-Delmotte, V., Jouzel, J.,
621 Barnola[3], J-M., Panno[5], L., Spahni, R., Tisserand, A., Siegenthaler, U., and Leuenberger, M.:
622 Anomalous flow below 2700 m in the EPICA Dome C ice core detected using $\delta^{18}O$ of atmospheric
623 oxygen measurements, Clim. Past, 3, 341-353, https://doi.org/10.5194/cp-3-341-2007, 2007.
624
625 Eisenstadt, D., Barkan, E., Luz, B., and Kaplan, A.: Enrichment of oxygen heavy isotopes during
626 photosynthesis in phytoplankton, Photosynth. Res., 103, 97-103,
627 https://doi.org/10.1007/s11120-009-9518-z, 2010.
628
629 Extier, T., Landais, A., Bréant, C., Prié, F., Bazin, L., Dreyfus, G., Roche, D. M., Leuenberger, M.: On
630 the use of $\delta^{18}O_{atm}$ for ice core dating, Quat. Sci. Rev., 185, 244-257,
631 https://doi.org/10.1016/j.quascirev.2018.02.008, 2018.
632
633 Guy, R. D., Fogel, M.L., and Berry, J. A.: Photosynthetic fractionation of the stable isotopes of oxygen
634 and carbon, Plant Physiol., 101, 37-47, https://doi.org/10.1104/pp.101.1.37, 1993.
635
636 Helman, Y., Barkan, E., Eisenstadt, D., Luz, B., and Kaplan, A.: Fractionation of the three stable
637 oxygen isotopes by oxygen-producing and oxygen-consuming reactions in photosynthetic
638 organisms, Plant Physiol., 138, 2292-2298, https://doi.org/10.1104/pp.105.063768, 2005.
639
640 Hillaire-Marcel, C., Kim, S-T., Landais, A., Ghosh, P., Assonov., S., Lécuyer, C., Blanchard, M., Meijer,
641 H. A. J., and Steen-Larsen, H.: A stable isotope toolbox for water and inorganic carbon cycle studies,
642 Nat. Rev. Earth Environ, 2, 699-719, https://doi.org/10.1038/s43017-021-00209-0 , 2021.
643
644 Hoffmann, G., Cuntz, M., Weber, C., Ciais, P., Friedlingstein, P., Heimann, M., Jouzel, J., Kaduk, J.,
645 Maier Reimer, E., Seibt, U., and Six, K.: A model of the Earth's Dole effect, Global Biogeochem. Cy.,
646 18, 1-15, https://doi.org/10.1029/2003GB002059, 2004.
647
648 Landais, A., Barkan, E., Yakir, D., and Luz, B.: The triple isotopic composition of oxygen in leaf water,
649 Geochim. Cosmochim. Ac., 70, 4105-4115, https://doi.org/10.1016/j.gca.2006.06.1545, 2006.
650
651 Landais, A., Dreyfus, G., Capron, E., Masson-Delmotte, V., Sanchez-Goñi, M. F., Desprat, S.,
652 Hoffmann, G., Jouzel, J., Leuenberger and M., Johnsen, S.: What drives the orbital and millennial

653 variations of $d^{18}O_{atm}$?, Quat. Sci. Rev., 29, 235-246, https://doi.org/10.1016/j.quascirev.2009.07.005,
654 2010.
655
656 Luz, B., and Barkan, E.: The isotopic composition of atmospheric oxygen, Global Biogeochem. Cy.,
657 25, GB3001, https://doi.org/10.1029/2010GB003883, 2011.
658
659 Luz, B., Barkan, E., Bender, M. L., Thiemens, M. H., and Boering, K. A.: Triple-isotope composition of
660 atmospheric oxygen as a tracer of biosphere productivity, Nature, 400, 547-550,
661 https://doi.org/10.1038/22987, 1999.
662
663 Malaizé, B., Paillard, D., Jouzel, J., and Raynaud, D.: The Dole effect over the Last two glacial-
664 interglacial cycles, J. Geophys. Res., 104, 14199-14208, https://doi.org/10.1029/1999JD900116,
665 1999.
666
667 Mehler, A.: Studies on reactions of illuminated chloroplasts: I. Mechanism of the reduction of
668 oxygen and other hill reagents, Arch. Biochem. Biophys., 33, 65–77,
669 https://doi.org/10.1016/00039861(51)90082-3, 1951.
670
671 Meijer, H. A. J., and Li, W. J.: The use of electrolysis for accurate $\delta^{17}O$ and $\delta^{18}O$ Isotope
672 Measurements in Water, Isot. Environ. Health Stud., 34, 349-369,
673 https://doi.org/10.1080/10256019808234072, 1998.
674
675 Milcu, A., Allan, E., Roscher, C., Jenkins, T., Meyer, S. T., Flynn, D., Bessler, H., Buscot, F.,
676 Engels, C., Gubsch, M., König, S., Lipowsky, A., Loranger, J., Renker, C., Scherber, C., Schmid,
677 B., Thébault, E., Wubet, T., Weisser, W. W., Scheu, S., and Eisenhauer, N.: Functionally and
678 phylogenetically diverse plant communities key to soil biota, Ecology, 94, 1878-1885,
679 https://doi.org/ 10.1890/12-1936.1, 2013.
680
681 Reutenauer, C., A. Landais, A., T. Blunier, T., C. Bréant, C., M. Kageyama, M., M.-N. Woillez, M-N.,
682 Risi, C., Mariotti, V., and P. Braconnot, Quantifying molecular oxygen isotope variations during a
683 Heinrich stadial, Clim. Past, 11, 1527-1551, https://doi.org/10.5194/cp-11-1527-2015, 2015.
684
685 Seltzer, A. M., Severinghaus, J. P., Andraski, B. J., and Stonestrom, D. A.: Steady state
686 fractionation of heavy noble gas isotopes in a deep unsaturated zone, Water Resour. Res., 53,
687 2716-2732, https://doi.org/10.1002/2016WR019655, 2017.

https://doi.org/10.5194/bg-2021-324
Preprint. Discussion started: 16 December 2021

688

689 Severinghaus, J. P., Beaudette, R., Headly, M. A., Taylor, K. and Brook, E. J.: Oxygen-18 of O_2 records
690 the impact of abrupt climate change on the terrestrial biosphere, Science, 324, 1431-1434,
691 https://doi.org/10.1126/science.1169473, 2009.

692

693 Shackleton, N. J.: The 100,000-Year Ice-Age Cycle Identified and Found to Lag Temperature,
694 Carbon Dioxide, and Orbital Eccentricity, Science, 289, 1897-1902,
695 https://doi.org/10.1126/science.289.5486.1897, 2000.

696

697 Sharp, Z. D., and Wostbrock, J. A. G.: Standardization for the Triple Oxygen Isotope System: Waters,
698 Silicates, Carbonates, Air, and Sulfates, Rev. Mineral. Geochem., 86, 179-196,
699 https://doi.org/10.2138/rmg.2021.86.05, 2021.

700

701 Stolper, D. A., Fischer, W. W., and Bender, M. L.: Effects of temperature and carbon source on the
702 isotopic fractionations associated with O_2 respiration for $^{17}O/^{16}O$ and $^{18}O/^{16}O$ ratios in *E.*
703 *coli*, Geochim. Cosmochim. Ac., 240, 152-172, https://doi.org/10.1016/j.gca.2018.07.039, 2018.

704

705 Wang, Y., Cheng, H., Lawrence Edwards, R., Kong, X., Shao, X., Chen, S., Wu, J., Jiang, X., Wang, X.,
706 and An, Z.: Millenial- and orbital-scale changes in the East Asian monsoon over the past 224,000
707 years, Nature, 451, 1090-1093, https://doi.org/10.1038/nature06692, 2008.